Contribution from the Departments of Chemistry, West Virginia University, Morgantown, West Virginia 26506, and Miami University, Oxford, Ohio 45056

Stereochemical Consequences of Deprotonation of the Bent Mo-H-Mo Bond in $Mo_2(\eta^5\text{-}C_5H_5)_2(CO)_4(\mu\text{-}H)(\mu\text{-}PMe_2)$

JEFFREY L. PETERSEN* and ROBERT P. STEWART, JR.*

Received June 29, 1979

A combined structural and spectroscopic study has been performed to examine the stereochemical consequences resulting from the deprotonation of the bent Mo-H-Mo bond in $Mo_2(\eta^5\text{-}C_5H_5)_2(CO)_4(\mu\text{-}H)(\mu\text{-}PMe_2)$. Deprotonation by treatment of the parent hydride with ethanolic KOH followed by the addition of tetraphenylarsonium chloride led to the isolation of $[Ph_4As]^+[Mo_2(\eta^5\text{-}C_5H_5)_2(CO)_4(\mu\text{-}PMe_2)]^-$. An X-ray diffraction analysis of the tetraphenylarsonium salt shows that the anion retains the basic overall configuration of the hydride with a pseudo-twofold axis passing through the bridging phosphido group which links the two $Mo(\eta^5\text{-}C_5H_5)(CO)_2$ units. A comparison of the appropriate bond distances and angles for the anion and hydride, however, reveals that several significant structural modifications occur upon deprotonation. The most evident one is the reduction of the Mo-Mo separation from 3.262 (2) Å in the hydride to 3.157 (2) Å in the anion. The averaged Mo-P bond distances are reduced by 0.06 Å, which suggests an increase in the Mo-P π-bonding contribution. The observed decrease in the Mo-C distances and increase in the C-O distances are consistent with increased charge delocalization into the π^* acceptor orbitals of the carbonyl groups. One CO group per Mo atom exhibits a small degree of semibridging behavior as indicated by the greater bending of these Mo-C-O bond angles and the 0.5-0.6 Å decrease in the corresponding Mo···C separations. These structural changes are reflected by the substantial upfield shift of the ^{31}P NMR resonance from 146.4 (hydride) to 61.6 ppm (anion) and the general decrease in ν_{CO} stretching frequencies for the anion. The ^{31}P chemical shifts support a significant metal-metal bonding component in both species. The tetraphenylarsonium salt of $[Mo_2(\eta^5\text{-}C_5H_5)_2(CO)_4(\mu\text{-}PMe_2)]^-$ anion crystallizes in a triclinic space group, $P\bar{1}$, with refined lattice parameters, $a = 10.346$ (3) Å, $b = 13.973$ (3) Å, $c = 14.571$ (3) Å, $\alpha = 101.38$ (2)°, $\beta = 101.53$ (2)°, $\gamma = 111.08$ (2)°, $V = 1840.5$ (7) Å^3, $d_{obsd} = 1.57$ g/cm^3, $d_{calcd} = 1.585$ g/cm^3, and $Z = 2$. Full-matrix least-squares refinement on F_o^2 of 2604 diffractometry data with $F_o^2 > 2\sigma(F_o^2)$ led to final discrepancy indices of $R(F_o) = 0.051$, $R(F_o^2) = 0.069$, and $R_w(F_o^2) = 0.107$ with $\sigma_1 = 1.79$.

Introduction

The stereochemistry of the bridging hydrogen atom in M-H-M bonds has been studied extensively by the application of X-ray and neutron diffraction methods to a wide variety of metal hydrides.[1] Generally, the protonation of a metal-metal bond is accompanied by a substantial increase in the metal-metal separation. In cases where an approximate position of the bridging H atom is not possible directly from difference Fourier maps, the variation in the metal-metal separation coupled with an examination of the ligand disposition about the metals can be used to estimate its location in the molecule. For example, the protonation of the Cr-Cr bond in the staggered D_{4d} $[Cr_2(CO)_{10}]^{2-}$ dianion leads to the formation of the eclipsed D_{4h} $[Cr_2(CO)_{10}(\mu\text{-}H)]^-$ monoanion.[2a] For this molecule, in which the H atom is the only bridging group, the Cr-Cr separation has been increased by ca. 0.4 Å from 2.97 to 3.39 Å. In trinuclear clusters[3] such as $[Re_3(CO)_{12}(\mu_2\text{-}H)_2]^-$ and $[Re_3(CO)_{12}(\mu\text{-}H)]^{2-}$ the approximate location of the bridging H atom was determined from the variation in the Re-Re distances from ca. 3.00 Å in the normal nonbridged Re-Re linkage to ca. 3.15 Å in the hydrido-bridged Re-H-Re bond and from the displacement of equatorial carbonyl ligands. Upon the basis of these examples, deprotonation of a M-H-M bond should be accompanied conversely by a decrease in the metal-metal separation. To investigate the structural effects which accompany the deprotonation of the Mo-H-Mo bond in $Mo_2(\eta^5\text{-}C_5H_5)_2(CO)_4(\mu\text{-}H)(\mu\text{-}PMe_2)$,[4] we have prepared and structurally characterized the tetraphenylarsonium salt of the isoelectronic $[Mo_2(\eta^5\text{-}C_5H_5)_2(CO)_4(\mu\text{-}PMe_2)]^-$ monoanion by X-ray diffraction methods. A combination of structural and spectroscopic (^{31}P NMR and IR) methods has permitted an assessment of the delocalization of the negative charge on the deprotonated anion and the nature of the metal-metal interaction.

* Address correspondence as follows: J.L.P., West Virginia University; R.P.S., Miami University.

Experimental Section

All manipulations were carried out in Schlenk apparatus under an atmosphere of dry nitrogen. All solvents (reagent grade) were dried by appropriate methods and were saturated with nitrogen prior to use. Infrared spectra were obtained on a Perkin-Elmer 180 spectrophotometer calibrated with carbon monoxide. Proton NMR spectra were recorded at 90.0 MHz on a Bruker WH-90DS spectrometer operating in the FT mode. Acetone-d_6 was used as solvent and internal Me_4Si served as reference. The $^{31}P\{^1H\}$ spectra were recorded on a Varian XL-100 spectrometer. Dry, degassed CH_2Cl_2 was used as solvent, and a probe containing acetone-d_6/H_3PO_4 (lock/reference) was inserted into the sample tube; positive chemical shifts are *downfield* from H_3PO_4. Attempts to obtain the ^{13}C NMR spectra of the hydride and the anion were unsuccessful due to their limited solubility. Microanalyses were performed by Galbraith Laboratories, Knoxville, TN.

Preparation of $Mo_2(\eta^5\text{-}C_5H_5)_2(CO)_4(\mu\text{-}H)(\mu\text{-}PMe_2)$. The hydride complex was prepared by the method of Hayter.[5] ν_{CO} infrared spectrum (CH_2Cl_2): 2017 (w), 1930 (vs), 1864 (s) cm^{-1} (lit.[5] (halocarbon mull): 2018 (m), 1930 (vs), 1859 (vs) cm^{-1}). ^{31}P NMR spectrum: 146.4 ppm (singlet).

Preparation of $[Ph_4As][Mo_2(\eta^5\text{-}C_5H_5)_2(CO)_4(\eta\text{-}PMe_2)]$. To a slurry of $Mo_2(\eta^5\text{-}C_5H_5)_2(CO)_4(\mu\text{-}H)(\mu\text{-}PMe_2)$ (627 mg, 1.26 mmol) in 12 mL of absolute ethanol was added 10.6 mL of a 0.239 M solution of ethanolic KOH. The mixture was heated at 40-50 °C for 1 h to give an intense red solution. The solution was filtered, and $[Ph_4As]Cl\cdot HCl\cdot 2H_2O$ (640 mg, 1.30 mmol) in 3 mL of absolute ethanol was added. The product separated as a red solid which was isolated on filtration and washed with ether (yield 728 mg, 66%). The

(1) (a) H. D. Kaesz and R. B. Saillant, *Chem. Rev.*, **72**, 231 (1972); (b) R. Bau and T. F. Koetzle, *Pure Appl. Chem.*, **50**, 55 (1978); (c) R. Bau, R. G. Teller, S. W. Kirtley, and T. F. Koetzle, *Acc. Chem. Res.*, **12**, 176 (1979).
(2) (a) L. B. Handy, J. K. Ruff, and L. F. Dahl, *J. Am. Chem. Soc.*, **92**, 7312 (1970); (b) J. Roziere, J. M. Williams, R. P. Stewart, Jr., J. L. Petersen, and L. F. Dahl, *ibid.*, **99**, 4497 (1977).
(3) M. R. Churchill, *Adv. Chem. Ser.*, **No. 167**, 36 (1978), and references cited therein.
(4) (a) J. L. Petersen, L. F. Dahl, and J. M. Williams, *J. Am. Chem. Soc.*, **96**, 6610 (1974); (b) J. L. Petersen and J. M. Williams, *Inorg. Chem.*, **17**, 1308 (1978).
(5) R. G. Hayter, *Inorg. Chem.*, **2**, 1031 (1963).

0020-1669/80/1319-0186$01.00/0 © 1980 American Chemical Society

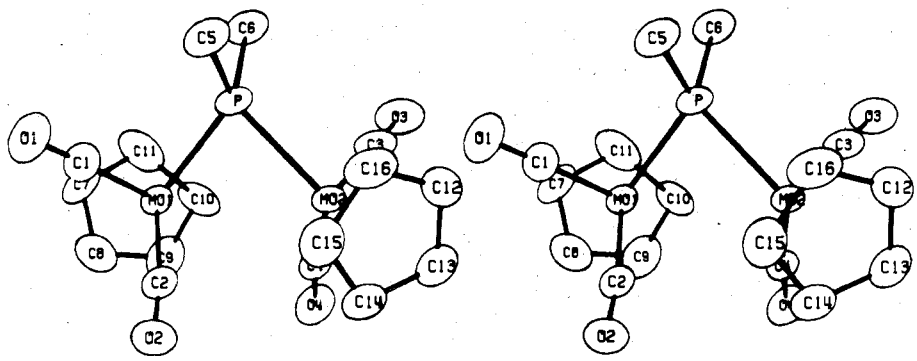

Figure 1. Stereographic drawing of the molecular configuration of the $[Mo_2(\eta^5\text{-}C_5H_5)_2(CO)_4(\mu\text{-}PMe_2)]^-$ anion with atom labeling. The thermal ellipsoids for this drawing are scaled to enclose 30% probability.

Table I. Unit Cell and Space Group Data for $[Ph_4As]^+[Mo_2(\eta^5\text{-}C_5H_5)_2(CO)_4(\mu\text{-}PMe_2)]^-$

cryst system	triclinic	d(obsd), g/cm^3	1.57
		d(calcd), g/cm^3	1.585
a, Å	10.346 (3)	Z	2
b, Å	13.973 (3)	μ, cm^{-1}	17.04
c, Å	14.571 (3)	range of transmissn coeff	0.80–0.85
α, deg	101.38 (2)		
β, deg	101.53 (2)	space group	$P\bar{1}$ (C_i^1, No. 2)
γ, deg	111.08 (2)	systematic absences	none
vol, Å^3	1840.5 (7)		
fw	878.50		

analytical sample was recrystallized from dichloromethane/ethanol. Anal. Calcd for $C_{40}H_{36}O_4PAsMo_2$: C, 54.67; H, 4.13; P, 3.53; As, 8.53. Found: C, 54.69; H, 4.32; P, 3.50; As, 8.32. ν_{CO} infrared spectrum (CH_2Cl_2): 1867 (m), 1826 (vs), 1771 (s), 1751 (m) cm^{-1}. ^{1}H NMR spectrum: τ 2.10 (C_6H_5, singlet), 5.19 (C_5H_5, singlet), 8.30 (CH_3, doublet, J_{PH} = 8.9 Hz). ^{31}P NMR spectrum: 61.6 ppm (singlet).

The Et_4N^+ salt was prepared similarly from $[Et_4N]Cl$. Anal. Calcd for $C_{24}H_{36}O_4PNMo_2$: C, 46.09; H, 5.80; P, 4.95; N, 2.24. Found: C, 45.82; H, 5.69; P, 4.95; N, 2.23. ν_{CO} infrared spectrum (CH_2Cl_2): 1868 (m), 1825 (vs), 1772 (s), 1748 (m) cm^{-1}. ^{1}H NMR spectrum: τ 5.15 (C_5H_5, singlet), 6.50 (CH_2, quartet, J_{HH} = 7.2 Hz), 8.27 (P-CH_3, doublet, J_{PH} = 9.0 Hz), 8.60 (CH_3, triplet of triplets, J_{HH} = 7.2 Hz, J_{NH} = 2.0 Hz).

Collection of X-ray Diffraction Data. A red, parallelepiped-shaped crystal of dimension 0.15 mm × 0.15 mm × 0.25 mm was mounted in a general orientation within a sealed thin-wall capillary tube and transferred to a Picker goniostat under computer control by a Krisel Control diffractometer automation system. A preliminary peak search for low-angle reflections produced a sufficient number of reflections for the autoindexing routine.[6,7] The initial lattice parameters indicated the Laue symmetry to be triclinic C_i-$\bar{1}$. From a rough orientation matrix the angular coordinates for higher order reflections were calculated and optimized by the automatic centering algorithm. The optimized angles (ω, χ, 2θ) from 20 centered diffraction peaks within a 2θ range of 25–31° gave the final lattice parameters in Table I. The experimental density was measured by flotation in a CCl_4/benzene solution.

Intensity data (hkl, $h\bar{k}l$, $hk\bar{l}$, $h\bar{k}\bar{l}$) were measured with Zr-filtered Mo Kα X-ray radiation (λ (Kα_1) 0.709 26 Å, λ (Kα_2) 0.713 54 Å) at a takeoff angle of 2° within a detector range of $3° \leq 2\theta \leq 40°$. The θ–2θ scan mode was employed to scan each peak at a fixed scan rate 2°/min. For each peak the scan width was determined from the expression 2.0 + 0.7 tan θ. Background counts of 10-s duration were measured at the extremes of each scan with the stationary-crystal, stationary-counter method. A scintillation counter was used with the pulse height analyzer adjusted to accept 90% of the diffraction peak. During data collection the intensities of three standard reflections were measured after every 120 min of exposure time. Their combined intensities decreased continually during data collection by 28%. This drop was attributed to a combination of crystal decay and the deterioriation of the diffraction tube. The intensity data were corrected for background, absorption, the nearly linear intensity decay, and Lorentz–polarization effects. The standard deviation for each of the 3467 measured peaks was calculated from the expression $\sigma^2(I) = \sigma_c^2(I) + (0.04I)^2$ where $\sigma_c^2(I) = w^2(S/t_s^2 + B/t_b^2)$ and $I = w(S/t_s - B/t_b)$. In these equations S represents the total scan count measured in time t_s, B is the combined background count in time t_b, and w is the scan width. Duplicate reflections were averaged to provide 2604 reflections with $F_o^2 \geq 2\sigma(F_o^2)$. No extinction correction was required.

Table II. Intensity Statistics for X-ray Diffraction Data of $[Ph_4As]^+[Mo_2(\eta^5\text{-}C_5H_5)_2(CO)_4(\mu\text{-}PMe_2)]^-$

		theoretical	
	exptl	centrosym	noncentrosym
E^2	1.000	1.000	1.000
MOD($E^2 - 1$)	0.937	0.968	0.736
MOD(E)	0.808	0.798	0.886

Structure Analysis. The approximate positions of the Mo, P, and As atoms were located from the first E map calculated by using the phase assignments for the set with the highest figure of merit from MULTAN 78.[8] The intensity statistics given in Table II are consistent with the centrosymmetric triclinic space group $P\bar{1}$ (C_i^1, No. 2). Subsequent Fourier and difference Fourier analyses provided the remaining nonhydrogen atom positions. Full-matrix least-squares refinement with anisotropic temperature factors for the 48 nonhydrogen atoms and fixed atom contributions[9,10] for the 36 hydrogen atoms converged with $R(F_o) = 0.051$, $R(F_o^2) = 0.069$, and $R_w(F_o^2) = 0.107$ with $\sigma_1 = 1.79$ for the 2604 reflections with $F_o^2 > 2\sigma(F_o^2)$.[11–15] On the last refinement cycle the maximum parameter shift to esd ratio was less than 0.20. A final difference Fourier showed residuals of about 1 e/Å^3 in the vicinity of the two Mo atoms. Presumably these features arise from the inadequacy of the model to account for the electron delocalization about the Mo atoms.

The final positional and thermal parameters for the nonhydrogen atoms are provided in Table III. Interatomic distances and bond angles with their esd's calculated from the errors of the fractional

(6) The algorithm written by L. Finger is based upon Jacobson's procedure.[7]
(7) R. A. Jacobson, *J. Appl. Crystallogr.*, **9**, 115 (1976).
(8) J. P. Declerq, D. Germain, P. Main, and M. M. Woolfson, *Acta Crystallogr., Sect. A*, **29**, 231 (1973).
(9) Idealized hydrogen positions located ca. 0.95 Å from the cyclopentadienyl, methyl, and phenyl carbons were calculated from MIRAGE.[10]
(10) J. C. Calabrese, MIRAGE, Ph.D. Thesis (Appendix II), University of Wisconsin, Madison, 1971.
(11) The least-squares refinements[12] of the X-ray diffraction data were based upon the minimization of $\sum w_i|F_o^2 - S^2F_c^2|$ where the individual weights, w_i, equal $1/\sigma^2(F_o^2)$ and S is the scale factor. The discrepancy indices were calculated from the expressions $R(F_o) = [\sum||F_o| - |F_c||/\sum|F_o|]$, $R(F_o^2) = \sum|F_o^2 - F_c^2|/\sum F_o^2$, and $R_w(F_o^2) = [\sum w_i|F_o^2 - F_c^2|^2/\sum w_i F_o^4]^{1/2}$. The final goodness-of-fit parameter is $\sigma_1 = [\sum w_i|F_o^2 - F_c^2|/(n-p)]^{1/2}$ where n is the number of observations and p is the number of parameters (viz., 433) varied. Final data-to-parameter ratio is 6:1.
(12) The scattering factors utilized in all calculations were those of Cromer and Mann[13] for the nonhydrogen atoms and those of Stewart et al.[14] for the hydrogen atoms with corrections included for anomalous dispersion.[15]
(13) D. T. Cromer and J. Mann, *Acta Crystallogr., Sect A*, **24**, 321 (1968).
(14) R. F. Stewart, E. R. Davidson, and W. T. Simpson, *J. Chem. Phys.*, **42**, 3175 (1965).
(15) D. T. Cromer and D. Liberman, *J. Chem. Phys.*, **53**, 1891 (1970).

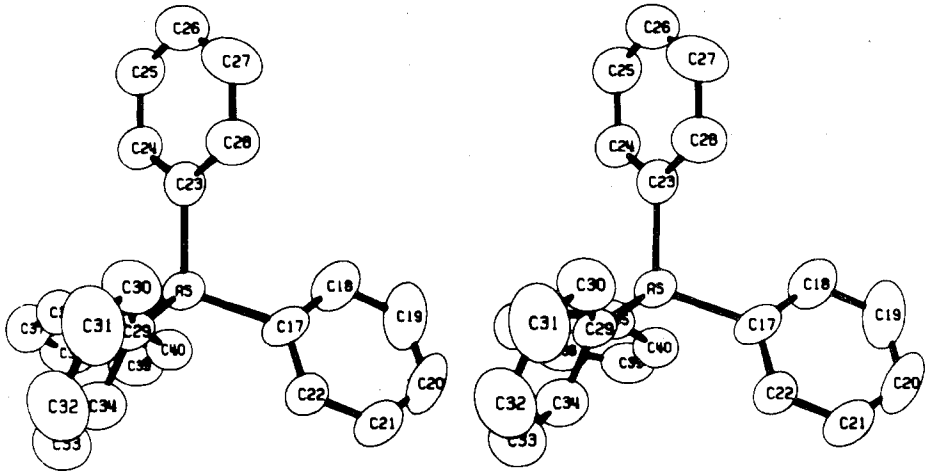

Figure 2. Stereoscopic view of the molecular configuration of the tetraphenylarsonium cation with atom labeling. The thermal ellipsoids are scaled to enclose 50% probability.

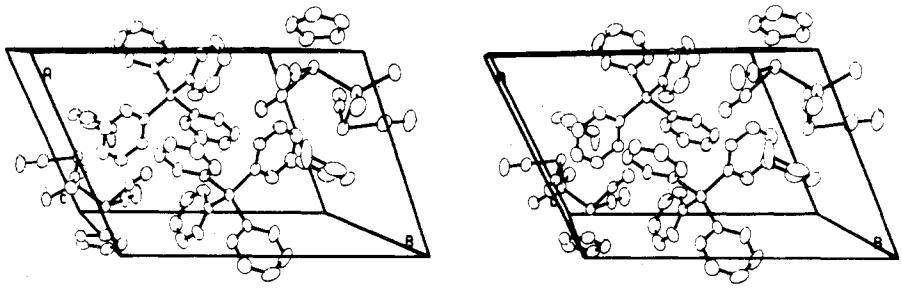

Figure 3. Stereoscopic view of the arrangment of two $[Ph_4As]^+$ cations and two $[Mo_2(\eta^5\text{-}C_5H_5)_2(CO)_4(\mu\text{-}PMe_2)]^-$ anions in the triclinic unit cell of symmetry $P\bar{1}$.

atomic coordinates are given in Table IV.[16,17] The hydrogen atom positions, least-squares planes of interest, and the observed and calculated structure factors are available.[18]

Results and Discussion

Description of the Crystal and Molecular Structure. The crystal structure consists of discrete μ-(dimethylphosphido)-bis[(η-cyclopentadienyl)dicarbonylmolybdate] anions, $[Mo_2(\eta^5\text{-}C_5H_5)_2(CO)_4(\mu\text{-}PMe_2)]^-$, and tetraphenylarsonium cations, $[Ph_4As]^+$. The molecular configurations of the anion and cation with their appropriate atom labeling schemes are depicted stereographically in Figures 1 and 2, respectively. The bond distances and angles tabulated in Table IV reflect the nearly C_2-2 symmetry of the anion with all corresponding pairs of distances and angles being equivalent within experimental error. The structure of the tetraphenylarsonium cation is typical with a nearly tetrahedral arrangement of four planar phenyl rings about the arsenic atom. The bond distances and angles (Table IV) agree with other structural determinations of the $[Ph_4As]^+$ cation.[19]

The arrangement of the two $[Ph_4As]^+$ cations and two $[Mo_2(\eta^5\text{-}C_5H_5)_2(CO)_4(\mu\text{-}PMe_2)]^-$ anions in the centrosymmetric triclinic unit cell is illustrated stereographically in Figure 3. The molecular packing is primarily dictated by van der Waals forces. The closest interionic contacts do not suggest any unusual interionic interactions.

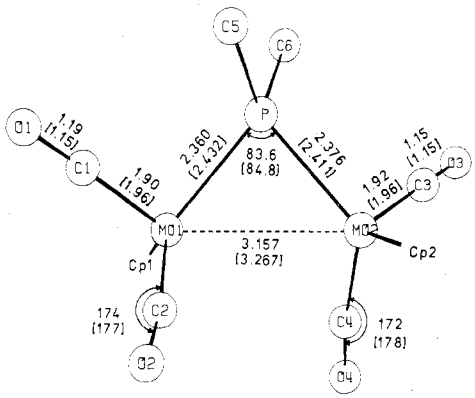

Figure 4. Comparison of selected molecular parameters between the $[Mo_2(\eta^5\text{-}C_5H_5)_2(CO)_4(\mu\text{-}PMe_2)]^-$ anion and $Mo_2(\eta^5\text{-}C_5H_5)_2(CO)_4(\mu\text{-}H)(\mu\text{-}PMe_2)$. The values for the hydride are given within the square brackets.

Comparison of the Structures of the $[Mo_2(\eta^5\text{-}C_5H_5)_2(CO)_4(\mu\text{-}PMe_2)]^-$ Anion and $Mo_2(\eta^5\text{-}C_5H_5)_2(CO)_4(\mu\text{-}H)(\mu\text{-}PMe_2)$. The overall geometries of the anion and the parent hydride are quite similar. Both species possess a pseudo-twofold axis which passes through the bridging groups that link the two $Mo(\eta^5\text{-}C_5H_5)(CO)_2$ moieties. In the hydride compound the spatial arrangement of the bridging hydrogen and phosphorus atoms and the two carbonyl ligands about each $Mo(C_5H_5)$ fragment resembles a "four-legged" stool with adjacent P and H legs. With the removal of the bridging hydrogen atom, the corresponding leg about each Mo atom is directed toward the overlap region in the resultant Mo–Mo bond. The twofold averaged bond angles between the adjacent legs of OC–Mo–CO, 80.3°, and P–Mo–CO, 83.9°, in the

(16) The computer programs which were used to perform the necessary calculations for the X-ray diffraction analysis with their accession names in the World List of Crystallographic Computer Programs are as follows: data reduction, DATALIB; data averaging and sort, DATASORT; Fourier summation, CNTFOR (modification of FORDAP); direct methods analysis, MULTAN 78; least-squares refinement, OR XFLS3; error analysis of distances and angles, OR FFE3; structural drawing, ORTEPII. Least-squares planes were calculated with the program PLNJO based upon the method of Blow.[17]

(17) D. Blow, *Acta Crystallogr.*, **13**, 168 (1960).

(18) Supplementary material.

(19) R. Bau, S. W. Kirtley, T. N. Sorrell, and S. Winarko, *J. Am. Chem. Soc.*, **96**, 988 (1974); F. A. Cotton and C. A. Murillo, *Inorg. Chem.*, **14**, 2467 (1975), and references cited therein.

Table III. Positional and Thermal Parameters ($\times 10^4$) for $[Ph_4As]^+[Mo_2(\eta^5\text{-}C_5H_5)_2(CO)_4(\mu\text{-}PMe_2)]^-$ [a,b]

atom	x	y	z	β_{11}	β_{22}	β_{33}	β_{12}	β_{13}	β_{23}
Mo1	6218 (1)	9219 (1)	1819 (1)	181 (2)	74 (1)	54 (1)	65 (1)	28 (1)	22 (1)
Mo2	9211 (1)	9026 (1)	2098 (1)	169 (2)	67 (1)	47 (1)	55 (1)	33 (1)	24 (1)
P	8033 (4)	9747 (2)	1035 (2)	214 (6)	72 (3)	49 (2)	63 (3)	31 (3)	26 (2)
C1	6458 (14)	10669 (11)	2029 (8)	235 (26)	103 (13)	64 (9)	90 (16)	26 (12)	14 (9)
C2	7193 (13)	9802 (9)	3212 (10)	161 (22)	70 (10)	71 (9)	47 (12)	33 (12)	33 (8)
C3	9008 (15)	8031 (10)	910 (9)	310 (29)	70 (11)	57 (9)	82 (15)	52 (13)	24 (8)
C4	7841 (13)	7747 (10)	2237 (8)	178 (22)	88 (11)	71 (9)	70 (14)	41 (11)	43 (8)
O1	6579 (12)	11566 (8)	2171 (7)	390 (24)	97 (9)	118 (8)	134 (13)	51 (11)	28 (7)
O2	7673 (9)	10184 (6)	4048 (6)	224 (17)	91 (8)	62 (6)	47 (9)	38 (8)	20 (6)
O3	8831 (13)	7398 (7)	195 (7)	483 (27)	110 (9)	78 (7)	144 (13)	95 (12)	22 (7)
O4	7134 (10)	6942 (8)	2369 (8)	221 (18)	105 (8)	170 (10)	63 (10)	80 (10)	97 (8)
C5	9005 (14)	11179 (9)	1154 (9)	228 (25)	79 (11)	106 (11)	52 (13)	44 (13)	51 (9)
C6	7490 (15)	9195 (10)	300 (8)	294 (29)	130 (13)	55 (9)	100 (16)	27 (13)	32 (9)
C7	3787 (16)	8549 (12)	994 (14)	180 (26)	130 (15)	115 (14)	77 (16)	−10 (15)	56 (12)
C8	3893 (17)	8187 (14)	1815 (11)	206 (28)	162 (18)	89 (12)	62 (19)	52 (15)	23 (12)
C9	4515 (15)	7462 (12)	1645 (14)	131 (24)	92 (13)	166 (17)	13 (14)	39 (15)	63 (12)
C10	5054 (25)	7473 (12)	884 (15)	697 (60)	119 (15)	181 (18)	241 (27)	293 (30)	100 (14)
C11	4377 (16)	8069 (14)	373 (10)	163 (25)	143 (17)	67 (10)	0 (16)	20 (13)	−28 (11)
C12	11733 (14)	9742 (14)	2596 (10)	184 (25)	134 (15)	81 (10)	78 (15)	50 (13)	37 (11)
C13	11259 (16)	9151 (11)	3195 (11)	224 (27)	100 (12)	100 (12)	85 (16)	36 (15)	48 (11)
C14	10580 (15)	9643 (12)	3726 (9)	192 (25)	119 (15)	50 (9)	63 (16)	4 (11)	23 (9)
C15	10693 (15)	10576 (11)	3456 (11)	199 (26)	79 (12)	70 (10)	52 (14)	−7 (13)	−15 (9)
C16	11383 (16)	10622 (12)	2740 (11)	174 (25)	96 (14)	88 (12)	9 (15)	5 (14)	42 (10)
As	2475 (1)	4999 (1)	3310 (1)	147 (2)	54 (1)	70 (1)	38 (1)	38 (1)	21 (1)
C17	1587 (14)	4249 (9)	4123 (10)	137 (22)	51 (10)	97 (11)	33 (13)	48 (12)	30 (8)
C18	2345 (14)	4493 (10)	5095 (12)	146 (23)	115 (13)	99 (12)	32 (14)	32 (14)	49 (11)
C19	1714 (20)	3864 (15)	5649 (11)	262 (33)	179 (19)	105 (12)	146 (22)	90 (18)	93 (14)
C20	391 (22)	3038 (13)	5256 (15)	246 (34)	114 (15)	148 (17)	92 (19)	146 (21)	79 (14)
C21	−359 (17)	2853 (10)	4308 (14)	248 (30)	63 (11)	126 (14)	28 (14)	104 (19)	25 (11)
C22	251 (16)	3450 (10)	3751 (9)	213 (27)	61 (10)	82 (10)	28 (14)	66 (14)	18 (9)
C23	3753 (15)	6429 (9)	4073 (8)	156 (23)	76 (10)	65 (8)	62 (14)	40 (11)	28 (7)
C24	5125 (16)	6885 (11)	4037 (9)	150 (23)	80 (12)	84 (10)	46 (14)	48 (13)	27 (9)
C25	5960 (14)	7953 (12)	4566 (10)	161 (23)	96 (14)	89 (11)	40 (16)	35 (13)	28 (10)
C26	5443 (20)	8548 (11)	5091 (10)	253 (33)	79 (12)	90 (11)	56 (18)	41 (16)	18 (9)
C27	4081 (20)	8094 (12)	5162 (10)	252 (32)	91 (15)	104 (12)	77 (18)	54 (17)	−2 (11)
C28	3223 (14)	7027 (11)	4646 (10)	177 (24)	87 (12)	103 (11)	46 (15)	62 (14)	10 (10)
C29	1027 (12)	4978 (10)	2258 (8)	164 (21)	47 (9)	67 (9)	27 (12)	31 (11)	21 (8)
C30	574 (16)	5809 (10)	2354 (10)	276 (29)	79 (12)	85 (10)	100 (16)	42 (15)	21 (9)
C31	−540 (21)	5705 (14)	1594 (14)	346 (38)	164 (19)	106 (13)	185 (23)	75 (19)	67 (14)
C32	−1210 (16)	4839 (17)	801 (12)	180 (26)	178 (20)	86 (12)	97 (20)	28 (14)	38 (13)
C33	−731 (19)	4053 (11)	717 (10)	259 (32)	95 (13)	85 (12)	57 (17)	31 (16)	21 (10)
C34	378 (16)	4103 (10)	1441 (11)	212 (26)	71 (12)	85 (10)	61 (14)	22 (14)	27 (10)
C35	3618 (12)	4319 (9)	2793 (8)	135 (20)	68 (10)	69 (9)	62 (11)	35 (11)	8 (8)
C36	4180 (16)	4633 (9)	2070 (10)	242 (27)	77 (11)	80 (10)	65 (15)	58 (14)	26 (9)
C37	5074 (17)	4198 (12)	1760 (10)	259 (30)	102 (13)	106 (12)	81 (17)	101 (15)	24 (11)
C38	5340 (16)	3458 (12)	2143 (12)	216 (29)	86 (13)	112 (13)	78 (16)	38 (15)	4 (11)
C39	4714 (17)	3101 (10)	2825 (11)	246 (29)	73 (11)	97 (11)	80 (16)	2 (15)	18 (10)
C40	3851 (14)	3551 (10)	3168 (9)	210 (24)	67 (10)	78 (9)	69 (14)	34 (12)	20 (8)

[a] The estimated standard deviations in parentheses for this and all subsequent tables refer to the least significant figures. [b] The form of the anisotropic temperature factor is $\exp[-(\beta_{11}h^2 + \beta_{22}k^2 + \beta_{33}l^2 + 2\beta_{12}hk + 2\beta_{13}hl + 2\beta_{23}kl)]$.

anion are somewhat larger than the respective averaged angles of 77.9 and 77.4° in the hydride due to the different steric and electronic requirements.

A comparison of the appropriate structural parameters for the anion and the hydride, as depicted in Figure 4, demonstrates that the deprotonation of the Mo–H–Mo bond produces several significant structural changes. The most evident one is the reduction of the Mo–Mo separation from 3.262 (2) to 3.157 (2) Å. This decrease is compatible with the replacement of the three-center, two-electron Mo–H–Mo bond upon deprotonation with a Mo–Mo bonding interaction. This 0.11 Å decrease is comparable to the observed differences between the bent, hydrogen-bridged Re–H–Re and the unbridged Re–Re bonds in the trinuclear anions[3,20] $[Re_3(CO)_{12}(\mu\text{-}H)_2]^-$ (Re–H–Re = 3.177 Å, Re–Re = 3.035 Å) and $[Re_3(CO)_{12}(\mu\text{-}H)]^{2-}$ (Re–H–Re = 3.125 Å, Re–Re = 3.016 Å). Since the bridging hydrogen atom in the parent hydride is not collinear with the two Mo atoms,[4] one expects the decrease in the metal–metal separation to be substantially less in a bent M–H–M bond than for a more linear one such as that in the $[Cr_2(CO)_{10}(\mu\text{-}H)]^-$ monoanion.[2,21] During the past several years, neutron diffraction studies[1] on a large number of metal hydrides have revealed a consistent pattern in bent M–H–M bonds. These bonds are described[1b,1c,22] as "closed" with the overlap region displaced from the H nucleus toward the centroid of the M–H–M triangle. This representation suggests the presence of a substantial metal–metal bonding component in the M–H–M bond. Consequently, the loss of a proton from the Mo–H–Mo linkage in the hydride would be expected to lead to a reduction in the metal–metal separation but not a substantial change in the overall geometry in the isoelectronic anion. The observed differences between these two structures (Figure 4) support this remark.

Since metal–metal distances are dependent upon the basic geometry of the compound and the appended ligands, the

(20) G. Ciani, G. D'Alfonso, M. Freni, R. Romiti, and A. Sironi, *J. Organomet. Chem.*, **157**, 199 (1978).

(21) The M–H–M angles in $Mo_2(\eta^5\text{-}C_5H_5)_2(CO)_4(\mu\text{-}H)(\mu\text{-}PMe_2)$ and $[Cr_2(CO)_{10}(\mu\text{-}H)]^-$ are 122.9 and 158.9°, respectively.

(22) J. P. Olsen, T. F. Koetzle, S. W. Kirtley, M. A. Andrews, D. L. Tipton, and R. Bau, *J. Am. Chem. Soc.*, **96**, 6621 (1974).

Table IV. Interatomic Distances (A) and Bond Angles (Deg) for $[Ph_4As]^+[Mo_2(\eta^5\text{-}C_5H_5)_2(CO)_4(\mu\text{-}PMe_2)]^-$ [a]

(A) Distances within $[Mo_2(\eta^5\text{-}C_5H_5)_2(CO)_4(\mu\text{-}PMe_2)]^-$

Mo1-P	2.360 (4)	Mo2-P	2.376 (4)
Mo1-C1	1.903 (16)	Mo2-C3	1.915 (13)
Mo1-C2	1.934 (13)	Mo2-C4	1.918 (12)
Mo1-C7	2.302 (14)	Mo2-C12	2.327 (13)
Mo1-C8	2.316 (16)	Mo2-C13	2.311 (16)
Mo1-C9	2.380 (15)	Mo2-C14	2.313 (11)
Mo1-C10	2.275 (14)	Mo2-C15	2.380 (12)
Mo1-C11	2.347 (12)	Mo2-C16	2.373 (12)
P-C5	1.841 (12)	P-C6	1.831 (12)
C1-O1	1.186 (20)	C3-O3	1.150 (15)
C2-O2	1.152 (15)	C4-O4	1.177 (16)
C7-C8	1.387 (28)	C12-C13	1.360 (24)
C8-C9	1.392 (29)	C13-C14	1.386 (25)
C9-C10	1.337 (32)	C14-C15	1.407 (24)
C10-C11	1.481 (31)	C15-C16	1.376 (25)
C11-C7	1.385 (27)	C16-C12	1.392 (28)
Mo1-Mo2	3.157 (2)	Mo2-Cp2(c)	2.024
Mo1-Cp1(c)	2.000		

(B) Distances within $[Ph_4As]^+$

As-C17	1.892 (15)	As-C29	1.905 (13)
C17-C18	1.382 (20)	C29-C30	1.392 (22)
C18-C19	1.388 (25)	C30-C31	1.370 (25)
C19-C20	1.350 (22)	C31-C32	1.343 (23)
C20-C21	1.365 (28)	C32-C33	1.352 (31)
C21-C22	1.360 (24)	C33-C34	1.395 (23)
C22-C17	1.342 (16)	C34-C29	1.371 (16)
As-C23	1.901 (10)	As-C35	1.937 (14)
C23-C24	1.348 (21)	C35-C36	1.372 (20)
C24-C25	1.385 (18)	C36-C37	1.376 (26)
C25-C26	1.340 (26)	C37-C38	1.353 (27)
C26-C27	1.356 (27)	C38-C39	1.371 (26)
C27-C28	1.384 (18)	C39-C40	1.378 (25)
C28-C23	1.390 (22)	C40-C35	1.370 (20)

(C) Bond Angles within $[Mo_2(\eta^5\text{-}C_5H_5)_2(CO)_4(\mu\text{-}PMe_2)]^-$

C1-Mo1-P	83.2 (5)	C3-Mo2-P	84.5 (5)
C2-Mo1-P	106.4 (4)	C4-Mo2-P	111.0 (4)
C1-Mo1-C2	79.2 (5)	C3-Mo2-C4	81.4 (6)
Mo1-P-C5	119.5 (5)	Mo2-P-C5	116.7 (4)
Mo1-P-C6	117.3 (5)	Mo2-P-C6	121.7 (6)
Mo1-P-Mo2	83.6 (1)	C5-P-C6	99.5 (6)
Mo1-C1-O1	178 (1)	Mo2-C3-O3	177 (1)
Mo1-C2-O2	174 (1)	Mo2-C4-O4	172 (1)
C11-C7-C8	108 (2)	C16-C12-C13	110 (2)
C7-C8-C9	105 (2)	C12-C13-C14	108 (2)
C8-C9-C10	114 (2)	C13-C14-C15	108 (1)
C9-C10-C11	102 (2)	C14-C15-C16	108 (2)
C10-C11-C7	108 (2)	C15-C16-C12	107 (2)
P-Mo1···Mo2	48.4 (1)	P-Mo2···Mo1	48.0 (1)
C1-Mo1···Mo2	111.9 (4)	C3-Mo2···Mo1	105.9 (5)
C2-Mo1···Mo2	74.6 (4)	C4-Mo2···Mo1	72.5 (5)
Cp1(c)[b]-Mo1-P	121.7	Cp2(c)-Mo2-P	122.2
Cp1(c)-Mo1-C1	124.0	Cp2(c)-Mo2-C3	123.6
Cp1(c)-Mo1-C2	127.3	Cp2(c)-Mo2-C4	121.6

(D) Bond Angles within $[Ph_4As]^+$

C17-As-C23	109.1 (5)	C23-As-C29	111.1 (6)
C17-As-C29	109.8 (6)	C23-As-C35	107.9 (6)
C17-As-C35	109.2 (6)	C29-As-C35	109.7 (5)
As-C17-C18	120 (1)	As-C29-C30	120 (1)
As-C17-C22	120 (1)	As-C29-C34	119 (1)
C22-C17-C18	120 (1)	C34-C29-C30	121 (1)
C17-C18-C19	118 (1)	C29-C30-C31	117 (1)
C18-C19-C20	121 (2)	C30-C31-C32	123 (2)
C19-C20-C21	119 (2)	C31-C32-C33	119 (2)
C20-C21-C22	121 (1)	C32-C33-C34	121 (1)
C21-C22-C17	121 (1)	C33-C34-C29	119 (2)
As-C23-C24	122 (1)	As-C35-C36	119 (1)
As-C23-C28	118 (1)	As-C35-C40	119 (1)
C28-C23-C24	120 (1)	C40-C35-C36	122 (1)
C23-C24-C25	118 (1)	C35-C36-C37	118 (1)
C24-C25-C26	122 (1)	C36-C37-C38	120 (2)
C25-C26-C27	120 (1)	C37-C38-C39	122 (2)
C26-C27-C28	119 (2)	C38-C39-C40	119 (2)
C27-C28-C23	121 (1)	C39-C40-C35	119 (1)

[a] The esd's given in parentheses for the interatomic separations and bond angles were calculated from the standard errors in the fractional coordinates of the corresponding atomic positions. [b] Cp1(c) and Cp2(c) refer to the centroids of the cyclopentadienyl rings.

Table V. ^{31}P NMR Data for Phosphido-Bridged Organometallic Compounds

ref	compd	δ[a]	nature of metal-metal interaction
26	$[Pd_3Cl(\mu\text{-}PPh_2)_2(PEt_3)_3][BF_4]$	204.8	Pd-Pd bond
27a	$[Ir(COD)(\mu\text{-}PPh_2)]_2$	166	Ir-Ir bond
28	$Fe_2(CO)_5(\mu\text{-}PPh_2)_2(\mu\text{-}CCPh)(PPh_3)$	155.4	Fe-Fe bond
this work	$Mo_2(\eta^5\text{-}C_5H_5)_2(CO)_4(\mu\text{-}H)(\mu\text{-}PMe_2)$	146.4	Mo-H-Mo bond
this work	$[Ph_4As][Mo_2(\eta^5\text{-}C_5H_5)_2(CO)_4(\mu\text{-}PMe_2)]$	61.6	Mo-Mo bond
27a	$[Rh(COD)(\mu\text{-}PPh_2)]_2$	−71	no Rh-Rh bond
26	$Pd_2Cl_2(\mu\text{-}PPh_2)_2(PEt_3)_2$	−127.3	no Pd-Pd bond
29	$Pt_2Cl_2(\mu\text{-}PPh_2)_2L_2$ L = PPr_3	−134.5	no Pt-Pt bond
	L = PEt_3	−135.4	
	L = PMe_2Ph	−136.9	
	L = $AsEt_3$	−142.5	
27b	L = PBu_3	−138.1	

[a] Ppm relative to H_3PO_4 external reference. Positive values are downfield from reference.

magnitude of the metal–metal separation may not necessarily provide a good criterion for verifying the existence of a direct electron-pair metal–metal bond.[23] The Mo–Mo distance of 3.157 (2) Å in the anion is considerably shorter than that of 3.235 (1) Å in $Mo_2(\eta^5\text{-}C_5H_5)_2(CO)_6$,[24] which contains a direct Mo–Mo bond. On the other hand, the smaller Mo–Mo distances for the $[Mo_2(CO)_{10}]^{2-}$ dianion (3.123 (7) Å)[2] and the doubly bridged molecules $Mo_2(CO)_8(\mu\text{-}PEt_2)_2$ (3.057 (6) Å)[25a] and $Mo_2(CO)_6(PEt_3)_2(\mu\text{-}PMe_2)_2$ (3.090 (2) Å)[25b] do not necessarily imply stronger metal–metal interactions but serve to show the range of observed Mo–Mo distances for compounds with different geometrical constraints and ligands.[23]

Another structural parameter which is appreciably affected is the Mo–P bond distance, which is on the average ca. 0.06 Å shorter in the anion. This decrease in the average Mo–P bond distance upon deprotonation suggests a significant increase in the Mo–P π-bonding contribution. The $^{31}P\{^1H\}$

(23) L. F. Dahl, E. Rodulfo de Gil, and R. D. Feltham, *J. Am. Chem. Soc.*, **91**, 1653 (1969).
(24) R. D. Adams, D. M. Collins, and F. A. Cotton, *Inorg. Chem.*, **13**, 1086 (1974).
(25) (a) L. R. Nassimbeni, *Inorg. Nucl. Chem. Lett.*, 7, 909 (1971); (b) R. H. B. Mais, P. G. Owston, and D. T. Thompson, *J. Chem. Soc. A*, 1735 (1967).

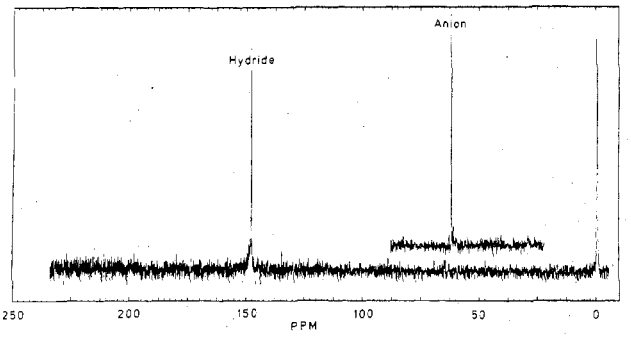

Figure 5. Proton-decoupled ^{31}P NMR spectra of the parent hydride, $Mo_2(\eta^5\text{-}C_5H_5)_2(CO)_4(\mu\text{-}H)(\mu\text{-}PMe_2)$, and tetraphenylarsonium salt of the $[Mo_2(\eta^5\text{-}C_5H_5)_2(CO)_4(\mu\text{-}PMe_2)]^-$ anion.

NMR spectra for the anion and the hydride, depicted in Figure 5, show that the phosphorus resonance is shifted significantly upfield from 146.4 (hydride) to 61.6 ppm (anion) due to the increased shielding of the ^{31}P nucleus in the anion. Although a limited amount of ^{31}P NMR data[26-29] is available for phosphido-bridged dimeric and polynuclear organometallic complexes (Table V), the ^{31}P resonance is particularly sensitive to its electronic environment as modified by the nature of the metal–metal interaction. Dixon and Rattray[26] observed that the ^{31}P resonance for the doubly bridging diphenylphosphido group in the $[Pd_3Cl(\mu\text{-}PPh_2)_2(PPh_3)_3]^+$ cation, which contains a Pd–Pd bond, is shifted downfield by over 330 ppm from that in $Pd_2Cl_2(\mu\text{-}PPh_2)_2(PEt_3)_2$, which does not contain a Pd–Pd bond. The presence of a metal–metal bond apparently results in a significant downfield shift of the ^{31}P resonance of the bridging phosphido group. The remaining NMR data in Table V support this relationship. For both the $[Mo_2(\eta^5\text{-}C_5H_5)_2(CO)_4(\mu\text{-}PMe_2)]^-$ anion and the parent hydride, the observed ^{31}P chemical shifts are consistent with the existence of a metal–metal interaction. The large upfield shift (85 ppm) of the ^{31}P resonance of the anion relative to that of the hydride probably reflects the enhancement of the Mo–P bond order. Clearly additional structural and NMR studies are necessary in order to further understand the relationship between the ^{31}P chemical shift and the nature of the M–P and M–M interactions in bridged M–P–M systems.

Finally, the structural parameters associated with the carbonyl groups reflect the delocalization of charge in the anion. The observed decrease in the Mo–C distances and increase in the C–O distances are consistent with increased charge delocalization into the π^*-acceptor orbitals of CO. This reduction in the CO bond order results in a general decrease in the ν_{CO} stretching frequencies for the anion.[30] A closer look at the Mo–C–O bond angles indicates that the Mo1–C2–O2 and Mo2–C4–O4 bond angles of 174 (1) and 172 (1)°, respectively, deviate more from linearity than the remaining two angles. This difference suggests that these carbonyl groups are exhibiting some slight semibridging character in the anion; i.e., C2 and C4 have moved toward Mo2 and Mo1, respectively. The Mo2···C2 and Mo1···C4 separations of 3.743 (5) and 3.735 (6) Å in the hydride are reduced to 3.234 (16) and 3.161 (16) Å, respectively, in the anion. It is possible that these distortions are responsible for the more complex ν_{CO} IR spectrum of the anion.

In summary, deprotonation of the bent Mo–H–Mo bond in $Mo_2(\eta^5\text{-}C_5H_5)_2(CO)_4(\mu\text{-}H)(\mu\text{-}PMe_2)$ reduces the Mo–Mo and Mo–P separations by 0.11 and 0.06 Å, respectively. The additional delocalization of charge into the π^*-acceptor orbitals of CO in the anion is accompanied by appropriate changes in the Mo–C and C–O bond distances. These structural changes are reflected by an 85-ppm upfield shift of the ^{31}P NMR resonance and a general decrease in the ν_{CO} stretching frequencies for the anion. Finally, one CO group per Mo atom exhibits weak semibridging character by shifting toward the site vacated by the proton.

Acknowledgment. The authors extend their appreciation to Dr. Jack D. Jamerson for obtaining the ^{31}P NMR spectra on the XL-100 NMR spectrometer at Union Carbide Technical Center, South Charleston, WV. Computer time for the refinement of the X-ray diffraction data was provided to J.L.P. by the West Virginia Network for Educational Telecomputing.

Registry No. $Mo_2(\eta^5\text{-}C_5H_5)_2(CO)_4(\mu\text{-}H)(\mu\text{-}PMe_2)$, 12092-01-2; $[Ph_4As][Mo_2(\eta^5\text{-}C_5H_5)_2(CO)_4(\mu\text{-}PMe_2)]$, 71948-54-4; $[Et_4N][Mo_2(\eta^5\text{-}C_5H_5)_2(CO)_4(\mu\text{-}PMe_2)]$, 71948-53-3.

Supplementary Material Available: Tables of structure factor amplitudes, hydrogen atom positions, and least-squares planes and a figure showing the infrared spectra of $[Mo_2(\eta^5\text{-}C_5H_5)_2(CO)_4(\mu\text{-}H)(\mu\text{-}PMe_2)]$ and $[Ph_4As][Mo_2(\eta^5\text{-}C_5H_5)_2(CO)_4(\mu\text{-}PMe_2)]$ (14 pages). Ordering information is given on any current masthead page.

(26) K. R. Dixon and A. R. Rattray, *Inorg. Chem.*, **17**, 1099 (1978).
(27) (a) P. E. Kreter, Jr., and D. W. Meek, paper presented at the 11th Central Regional Meeting of the American Chemical Society, Columbus, OH, May 1979; see Abstracts, No. INOR 4, p 64; (b) P. E. Kreter, Jr., and D. W. Meek, private communication.
(28) Private communication to J. D. Jamerson (Union Carbide) from A. J. Carty (University of Guelph, Waterloo, Ontario, Canada).
(29) C. Eaborn, K. J. Odell, and A. Pidcock, *J. Organomet. Chem.*, **170**, 105 (1979).
(30) Infrared spectra are provided in the supplementary material.